A CRITERION FOR BIAXIAL FATIGUE OF MILD STEEL AT LOW ENDURANCE

D.G. HAVARD,
Ontario Hydro Research Laboratories, Toronto, Ontario,

T.H. TOPPER,
Department of Civil Engineering,
University of Waterloo, Waterloo, Ontario, Canada

ABSTRACT

Results of a program of fatigue tests on mild steel are reviewed. Uniaxial, torsional and five biaxial stress states were applied with full reversal and principal strain control. The plastic strain and stable stress range data are related to fatigue life by the Coffin-Manson and Basquin laws. The slopes of the Coffin-Manson curves depend on stress ratio according to a relation based on the energy imparted to the planes of maximum shear stress. Stable cyclic stress-plastic strain curves for each stress ratio are normalized using octahedral stresses and strains.

Fatigue strength at 10^4 cycles can be adequately described, in terms of stable stress, by a modified maximum shear stress criterion. This criterion includes a small influence of the stress normal to the plane of maximum shear. From these relations a criterion is developed which predicts fatigue life from range of principal strain for all stress states. Comparison of the experimental data with other criteria presently in use reveals non-conservative discrepancies. The proposed criterion offers significant improvement.

1. INTRODUCTION

In nuclear and fossil-fuel fired thermal generating stations, as well as in a number of other industrial applications, many components are subjected to a significant cyclic loading a relatively few times during the service life. The major load cycle would be associated with a start-up, a period of operation, possibly at elevated temperature and a shutdown of the plant. The nominal stresses will in general follow a similar pattern of an increase, maintenance for some time with a possibility of relaxation, followed by a decrease.

Fatigue occurs in critical locations of such components where some local plasticity occurs during each application of load. These critical locations may be in the surface at notches, discontinuities, or welds; or they may be internal at a flaw or inclusion. The plastic deformation zone, occurring in a

region of high stress gradient, is restricted by the surrounding elastic region. In the small plastic zone, the mean stress due to the zero to maximum service loading cycle is relaxed to close to zero by the cyclic plasticity. Subsequently, the stresses are fully-reversed while the strain fluctuates about a mean strain that is small enough not to affect the fatigue life. The flaws or discontinuities at which fatigue cracks initiate are most commonly found at a free surface. Here the stress state approaches biaxiality because the stress normal to the surface is comparatively small.

However, tests to evaluate the fatigue properties of materials are for convenience most often performed under uniaxial stress conditions. Relationships to permit application of such fatigue data to the practical biaxial stress state are required to properly evaluate the fatigue resistance of most structural components.

2. BIAXIAL FATIGUE CRITERIA

Criteria that can be applied to cyclic biaxial stressing in the range to cause failure at lives in excess of 10^6 cycles have been developed in a number of earlier studies, for example by Gough [1], Findley [2], Marin [3] and Sawert [4]. The criteria developed are analogous to those applicable to yielding of metals under biaxial direct stress. The distortion strain energy and maximum shear stress criteria are generally favoured for ductile metals with neither showing clear superiority due to the normal scatter present in the experimental data. For metals which contain numerous internal discontinuities, and hence in which the fatigue process consists predominantly of crack propagation, Sawert [4] and Crosby et al [5] showed that the maximum principal stress criterion provides good correlation.

.....

LIST OF SYMBOLS

A, B, C, k', K_1	parameters	U_T	energy imparted to all planes
		α	axial to circumferential stress ratio
b	slope of Basquin curve	Δ	range
c	slope of Coffin-Manson curve	ϵ	strain
E	Young's modulus	$\bar{\epsilon}_p$	octahedral plastic strain
m	fraction of sum of stresses modifying shear stress	ν	Poisson's ratio
		σ	stress
n'	cyclic strain hardening exponent	σ^*	equivalent stress according to modified shear stress theory
N_f	number of cycles at fracture	$\bar{\sigma}$	octahedral stress
U_s	energy imparted to planes of maximum shear		

SUBSCRIPTS

1, 2, 3	principal directions	o	at 10^4 cycles
e, p	elastic, plastic	u	uniaxial

Biaxial fatigue in the short life range has not been studied in sufficient detail to provide a criterion that can be generally used with confidence. Pascoe et al [6] have shown that the fatigue behaviour of two steels under four states of biaxial stress does not correspond to the conventional yield criteria while Taira et al [7] suggest the use of the distortion strain energy theory applied to strain range. The ASME Boiler and Pressure Vessel Code (Section III) [8] employs a method developed by Langer [9] based on the maximum shear stress theory.

3. STUDY OF BIAXIAL FATIGUE OF MILD STEEL

In the present paper a new criterion is developed based on biaxial fatigue data, shown in Table 1, from a recent study of normalized 1018 steel by the authors [10]. The data were generated under fully reversed, strain controlled cyclic loading conditions using uniaxial, torsional and five biaxial stress states. The equipment designed to apply fully reversed biaxial loading to thin-walled cylindrical specimens has been described previously [11]. The instrumentation system permitted continuous monitoring of both stresses and strains throughout the test. The tests were terminated when a small crack was apparent from a distortion of the hysteresis loop thus excluding most of the propagation stage from the fatigue life data. The fatigue lives obtained were between 2000 and 100,000 cycles. The specimens were tested in hydraulic oil and at room temperature. The data in Table 1 are the controlled principal strain range $\Delta\epsilon_1$, the corresponding principal stress range at 50 per cent of the fatigue life, $\Delta\sigma_1$, at which point the material is considered to have stabilized following the initial cyclic hardening or softening behaviour, and the number of cycles to failure N_f.

4. FATIGUE LIFE AS A FUNCTION OF ELASTIC AND PLASTIC STRAIN RANGES

For each stress state the elastic strain range, $\Delta\epsilon_{1e}$, and the stress range are related through the generalized Hooke's law. When the axial strain was used for control this gives:

$$\Delta\epsilon_{1e} = \frac{\Delta\sigma_1}{E}(1 - \frac{\nu}{\alpha}) \qquad (1)$$

where α is the axial to circumferential stress ratio, and E and ν are the Young modulus and Poisson's ratio respectively. The plastic strain range in the direction of control, $\Delta\epsilon_{1p}$, is then given by:

$$\Delta\epsilon_{1p} = \Delta\epsilon_1 - \Delta\epsilon_{1e} \qquad (2)$$

The ranges of total, plastic, and elastic strain in the direction of control were obtained using (1) and (2) and similar expressions for circumferentially controlled tests. These are plotted against fatigue life in Figure 1. Simple power laws have been used to relate fatigue life to stable values of plastic strain range by Coffin [12] and Manson [13] and of stress range by Basquin [14]. Thus the total strain range may be represented by the sum of two power functions of the fatigue life namely:

$$\Delta\epsilon_1 = \Delta\epsilon_{1e} + \Delta\epsilon_{1p} = AN_f^b + BN_f^c \qquad (3)$$

where the data are fully represented by four independent parameters A, B, b and c.

Lines corresponding to such power laws for elastic, plastic and total strain range have been fitted to each series of data with least squares deviation and are included in the figure. These are seen to adequately represent the experimental values.

5. CONTOURS OF FATIGUE LIFE

Figure 2 shows contours of equal fatigue life at 10^4 cycles obtained from the experimental data on the bases of total, plastic, and elastic components of principal strain. Data are shown only between lines representing principal strain ratios (and coincidentally stress ratios) of 1.00 and -1.00 which form axes of symmetry for isotropic materials. The data shown in the figure for stress ratios of 0.50 and -0.34 would normally appear outside these axes of symmetry as the circumferential stress is greater than the axial stress. The data from the uniaxial tests, performed on samples cut either parallel or transverse to the axis of the parent forging, indicate that the material is isotropic at the fatigue lives of interest. Thus these data have been transferred to the positions of the inverse values of stress ratios as shown, to facilitate direct comparisons.

Figure 2 also includes the shapes of contours of equal fatigue life according to the distortion strain energy, the maximum stress, maximum strain and maximum shear-stress failure criteria. Comparison of the shape of the experimentally obtained contours of equal fatigue life indicates that none of the failure criteria describes the contours based on total strain or on plastic strain.

6. MODIFIED MAXIMUM SHEAR STRESS CRITERION

The shape of the contour based on elastic strain range does show similarities to that of the maximum shear theory. This theory provides a reasonable fit for negative stress ratios but shows considerable deviation from the data for positive stress ratios. The difference between these contours suggests a modification to the criterion that has increasing effect as the strain ratio increases from -1.00 to 1.00. For biaxial conditions, the sum of the two principal stresses fulfills this condition. This modification corresponds to the stress normal to the plane of maximum shear. A similar criterion was suggested by Stanfield [15].

This modified maximum shear stress criterion may be expressed algebraically in terms of the principal stress ranges as follows:

$$\frac{\Delta\sigma_1}{2} + m(\Delta\sigma_1 + \Delta\sigma_2) = C \qquad (4a)$$

for positive stress ratios and

$$\frac{\Delta\sigma_1 - \Delta\sigma_2}{2} + m(\Delta\sigma_1 + \Delta\sigma_2) = C \qquad (4b)$$

for negative stress ratios, where C is a constant for any specified life and m is the fraction of the sum of the stress ranges.

If the stress range causing fatigue failure in uniaxial tests is denoted by $\Delta\sigma^*$, and noting that $\Delta\sigma_2 = \frac{\Delta\sigma_1}{\alpha}$ (4)

becomes $\Delta\sigma_1(1 + \frac{2m}{\alpha(2m+1)}) = \Delta\sigma^*$ (5a)

for positive stress ratios and

$$\Delta\sigma_1(1 + \frac{2m-1}{\alpha(2m+1)}) = \Delta\sigma^* \qquad (5b)$$

for negative stress ratios.

This modified maximum shear stress criterion has been presented earlier [10]. It offers a simple relationship for the effect of biaxiality on fatigue life that is convenient and sufficiently accurate for design purposes provided the true stresses can be determined.

7. STRESS-STATE DEPENDENCE OF COFFIN-MANSON SLOPE

The slopes of the logarithmic plots of plastic strain range versus fatigue life can be observed in Figure 1. The numerical values for these slopes, which are included as parameter c in Table 1, show that the slope is dependent upon the stress state and has values between -0.546 and -0.259. This dependence on stress state has been noted by other workers (Pascoe et al [6], Libertiny [16]) who have attempted to correlate the variation of slope with stress or strain parameters. The values of the slopes are plotted against stress ratio in Figure 3, which also includes comparable values from other studies of fatigue of mild steel under more than one stress state.

The data points from this study are in reasonable agreement with those of Pascoe and de Villiers and show some difference notably in torsion, with data from Yokobori [17]. While there have been other studies of the fatigue behaviour of mild steel in the low cycle range under more than one stress condition, the plastic strain range was seldom measured and so additional comparable slope values are not available. Figure 3 includes curves representing the relationships used by Pascoe and Libertiny to correlate such slopes with stress state.

8. RELATION FOR COFFIN-MANSON SLOPE

The figure also includes a curve developed in this study which offers both a reasonable fit to the data points and an interpretation based on energy principles for the variation of slope. It is hypothesized that the part of the input energy which is directly applied to the planes of maximum shear stress in each stress ratio governs the slope of the Coffin-Manson line.

The total energy required to develop principal strains ϵ_1, ϵ_2 and ϵ_3 is given by:

$$U_T = \frac{1}{2}(\sigma_1 \epsilon_1 + \sigma_2 \epsilon_2 + \sigma_3 \epsilon_3). \qquad (6)$$

By assuming that the volume remains constant and setting $\sigma_2 = \frac{\sigma_1}{\alpha}$ and $\sigma_3 = 0$ (6) simplifies to: $$U_T = \frac{1}{2}\lambda\sigma_1^2\frac{(1-\alpha+\alpha^2)}{\alpha^2} . \quad (7)$$

For positive stress ratios the greatest values of shear stress and hence also of shear strain are in the two shear planes that intersect the surface at 45 degrees. The energy absorbed in shear deformation in the direction of these two planes, U_s, is given by: $$U_s = \frac{3}{8}\lambda\sigma_1^2(1 + \frac{1}{\alpha^2}) . \quad (8)$$

For negative stress ratios the maximum shear is in the plane normal to the surface, which is at 45 degrees to the σ_1 and σ_2 axes. For this plane the energy absorbed in shear is given by: $$U_s = \frac{3}{8}\lambda\sigma_1^2\frac{(1-\alpha)^2}{\alpha^2} . \quad (9)$$

It is now postulated that the value of the Coffin-Manson slope, c, is determined by: $$c\frac{U_s}{U_T} = \text{constant.} \quad (10)$$

This reduces to $$c = c_u\frac{1-\alpha+\alpha^2}{1+\alpha^2} \quad (11a)$$

for positive stress ratios and $$c = c_u\frac{1-\alpha+\alpha^2}{(1-\alpha)^2} \quad (11b)$$

for negative stress ratios, where c_u is the slope for the uniaxial stress state. Curves representing these two expressions are included in Figure 3 where they are seen to provide a better fit to the data than either of the two earlier hypotheses.

9. CYCLIC STRESS-STRAIN BEHAVIOUR

The stress-strain curve of a material is dependent on its history of loading and hence throughout cyclic loading tests there is a continuous change in the shape of this curve. The curve for material with no prior loading history is that obtained in a monotonic tension test. In cyclic loading tests on most materials, progressive deviations from this curve take place at a decreasing rate until at some late stage prior to fatigue failure a substantially stable stress-strain curve is attained. The curve at 50 per cent of the fatigue life is generally used as representing this stable state. It has been used here to permit the effects of stress ratio on this property to be examined.

The curves were obtained in this study using the measurements of stress and strain range taken on each specimen during the biaxial fatigue tests. The plot of stress range at 50 per cent of the fatigue life against total strain range for each specimen of each test series was taken to represent the stable cyclic stress-strain curve. These values are included in Table 1.

These stress-strain curves can be represented by the sum of a power law term for plastic strain (the Ramberg-Osgood relationship [18]) and a linear term for elastic strain.

For the biaxial case, with stress ratio α, this becomes

$$\Delta\epsilon_1 = \frac{\Delta\sigma_1(1-\frac{\nu}{\alpha})}{E} + k' \frac{\Delta\sigma_1}{50}^{\frac{1}{n'}} . \qquad (12)$$

To produce coefficients that are less dependent on each other, the term describing plastic strain includes stress range as a ratio of 50 ksi, which falls within the range of data for almost all tests. The values of parameters k' and n' obtained from these plots are listed in Table 1.

10. DEPENDENCE OF CYCLIC STRESS-STRAIN BEHAVIOUR ON STRESS STATE

The cyclic stress-strain behaviour for the eight stress states was found to be normalized by the generalized Hooke's law for the elastic strains and the use of deviatoric stresses and plastic strains. For the biaxial stress state, the ranges of deviatoric plastic strain, $\Delta\bar{\epsilon}_p$, and deviatoric stress, $\Delta\bar{\sigma}$, are given by

$$\Delta\bar{\epsilon}_p = \frac{2\,\Delta\epsilon_{1p}\sqrt{1-\alpha+\alpha^2}}{2\alpha-1} \qquad (13)$$

and

$$\Delta\bar{\sigma} = \Delta\sigma_1 \frac{\sqrt{1-\alpha+\alpha^2}}{\alpha} . \qquad (14)$$

Figure 4 shows that these data do form a reasonably compact band, when plotted on this basis. However, some sets of data, notably from the torsion tests and the tests at 3.89 stress ratio, deviate from the majority. For values of equivalent plastic strain between 0.001 and 0.01, which includes the data for all stress ratios, 90 per cent of the data points fall within 14 per cent of the best fit straight line. This generalized cyclic stress-plastic strain curve is designated in subsequent analysis by

$$\Delta\bar{\epsilon}_p = K_1 \Delta\bar{\sigma}^{\frac{1}{n'}} . \qquad (15)$$

11. INTERRELATIONSHIP BETWEEN PARAMETERS

Halford has shown [19] that the slopes of the Coffin-Manson curve, c, the Basquin curve, b, and of the cyclic stress-plastic strain curve, 1/n', are related by

$$n'c = b. \qquad (16)$$

This relationship is based on the assumption that the cyclic stress-strain curve, as defined by the stable locus of the loop tips for a series of tests at different strain ranges, is geometrically similar to the loading path described by the profile of the hysteresis loops at this stable condition.

The equations developed above are sufficient to produce a relationship for fatigue life under repeated biaxial stress in terms of applied total strain range. This strain range can be obtained either by measurement on a structure or by calculation using elastic theory as presently used in the ASME Code [8].

12. BIAXIAL FATIGUE RELATION BASED ON STRAIN

The elastic component of the principal strain range that will produce fatigue failure in N_f cycles is obtained by combining (1), (3), (5), (11) and (16):

(8)

$$\Delta\epsilon_{1e} = \frac{\Delta\sigma_o^*}{E}\frac{(\alpha-\nu)}{(\alpha+\frac{2m}{2m+1})}\left(\frac{N_f}{10^4}\right)^{-n'c_u}\frac{(1-\alpha+\alpha^2)}{(1+\alpha^2)} \tag{17a}$$

for positive stress ratios and

$$\Delta\epsilon_{1e} = \frac{\Delta\sigma_o^*}{E}\frac{(\alpha-\nu)}{(\alpha-\frac{2m-1}{2m+1})}\left(\frac{N_f}{10^4}\right)^{-n'c_u}\frac{(1-\alpha+\alpha^2)}{(1-\alpha)^2} \tag{17b}$$

for negative stress ratios where $\Delta\sigma_o^*$ is the range of equivalent stress according to (5) at 10^4 cycles.

The equivalent forms for the principal plastic strain range are obtained from (3), (5), (11), (13), (14), (15) and (16):

$$\Delta\epsilon_{1p} = K_1(\alpha-\tfrac{1}{2})(1-\alpha+\alpha^2)^{\left(\frac{1}{2n'}-\frac{1}{2}\right)}\left(\frac{\Delta\sigma_o^*}{\alpha+\frac{2m}{2m+1}}\right)^{\frac{1}{n'}}\left(\frac{N_f}{10^4}\right)^{\frac{-c_u(1-\alpha+\alpha^2)}{(1+\alpha^2)}} \tag{18a}$$

for positive stress ratios and

$$\Delta\epsilon_{1p} = K_1(\alpha-\tfrac{1}{2})(1-\alpha+\alpha^2)^{\left(\frac{1}{2n'}-\frac{1}{2}\right)}\left(\frac{\Delta\sigma_o^*}{\alpha+\frac{2m-1}{2m+1}}\right)^{\frac{1}{n'}}\left(\frac{N_f}{10^4}\right)^{\frac{-c_u(1-\alpha+\alpha^2)}{(1-\alpha)^2}} \tag{18b}$$

for negative stress ratios.

The principal total strain range is then the sum of its elastic and plastic components obtained from (17) and (18).

Five independent coefficients, c_u, n', k, m and K_1, occur in this expression for the principal total strain range. The values for these coefficients which provide the least squares best fit to the separated values of total, plastic and elastic strain range for each fatigue life and stress ratio have been evaluated numerically. The resulting equation for the maximum principal total strain range is as follows:

$$\Delta\epsilon_1 = 2.44\times10^{-3}\frac{(\alpha-0.28)}{(\alpha+0.038)}\left(\frac{N_f}{10^4}\right)^{\frac{-0.1713(1-\alpha+\alpha^2)}{(1+\alpha^2)}}$$

$$+2.37\times10^{-8}(\alpha-0.5)(1-\alpha+\alpha^2)^{0.928}\left(\frac{73.2}{\alpha+0.038}\right)^{2.856}\left(\frac{N_f}{10^4}\right)^{\frac{-0.489(1-\alpha+\alpha^2)}{(1+\alpha^2)}} \tag{19a}$$

for positive stress ratios and

$$\Delta\epsilon_1 = 2.44\times10^{-3}\frac{(\alpha-0.28)}{(\alpha-0.924)}\left(\frac{N_f}{10^4}\right)^{\frac{-0.1713(1-\alpha+\alpha^2)}{(1-\alpha)^2}}$$

$$+2.37\times10^{-8}(\alpha-0.5)(1-\alpha+\alpha^2)^{0.928}\left(\frac{73.2}{\alpha-0.924}\right)^{2.856}\left(\frac{N_f}{10^4}\right)^{\frac{-0.489(1-\alpha+\alpha^2)}{(1-\alpha)^2}} \tag{19b}$$

for negative stress ratios. This equation describes a surface representing the larger principal strain range as a function of stress ratio and fatigue life. Its separate terms describe equivalent surfaces for plastic and elastic strain ranges.

13. COMPARISON WITH EXPERIMENTAL DATA

The degree to which these expressions represent the data is indicated in Figure 1 where sections through these three surfaces are compared to the measured data points. The data, when transformed into ratios of measured to calculated strain range, are distributed normally about the fitted surfaces. Sixty per cent of the measured strain range values are within 12 per cent of the calculated values, and 90 per cent of the data within 23 per cent.

The correspondence with the individual data points is best for the elastic strains and poorest for the plastic strains. The generalized equation underestimates the fatigue life for the data obtained at a stress ratio of 1.21. For 0.50 stress ratio, the equation overestimates the fatigue life. These errors of fit are larger at the shorter fatigue lives investigated. The discrepancy in this part of the domain is the most serious divergence from the data. It indicates the need for additional fatigue testing under positive stress ratios at strain ranges to produce failure in 10^3 to 10^4 cycles.

Contours of equal fatigue life according to (19), showing the influence of stress ratio on fatigue behaviour based on total strain range and on stable stress range, are given in Figures 5 and 6. These figures also include mean and scatter band width data, interpolated from the experimental values, corresponding to fatigue lives of 10^3, 10^4 and 10^5 cycles. The contours of each figure show progressive variation with fatigue life. All other theories that have been used give contours that are geometrically similar for each fatigue life. The difference in the appearance of these equivalent sets of contours emphasizes that cyclic strains of sufficient amplitude to cause low cycle fatigue are related to stresses through non-linear laws.

14. PREDICTED FATIGUE LIFE CONTOURS BASED ON STRAIN

The contours of Figure 5 indicate that for maximum principal strain ranges above 0.003, the shortest fatigue life occurs under the equibiaxial stress state. On the other hand, the data points for this range of strains indicate that the most damaging biaxial stress state is at a stress ratio of around 0.5. At principal strain ranges below 0.003, both the contours and the data points show that the torsional fatigue tests give the shortest lives. They also show that, at all principal strain ranges studied, uniaxial stressing is the least damaging biaxial state.

The data points in Figure 5 indicate the range of the effect of stress ratio on fatigue life at constant maximum principal strain range. The ratio of maximum to minimum fatigue life varies from about 3 at the longest to more than 30 at the shortest fatigue lives studied.

15. PREDICTED FATIGUE LIFE CONTOURS BASED ON STRESS

When the loading condition is expressed in terms of stable stresses, the contours and interpolated test data shown in Figure 6 describe the influence of biaxiality. The data points indicate that at constant maximum principal stress range, the longest fatigue lives occur under uniaxial stressing. The

contours are in agreement with this at the shorter lives studied. However, as the fatigue life increases from 10^4 to 10^5 cycles, they show slightly longer fatigue lives at increasing values of positive stress ratio. At 10^5 cycles, the least damaging stress ratio is about 0.8.

For all fatigue lives, the most damaging stress ratio for each value of maximum principal stress range is pure shear loading. At each value of maximum principal stress range, the ratio of maximum to minimum fatigue life due to biaxiality is over 100 throughout the life range investigated.

16. COMPARISON OF EXPERIMENTAL DATA WITH OTHER BIAXIAL CRITERIA

It is pertinent to compare data of this study with the predictions of this generalized biaxial equation and of other procedures in common use. Alternative criteria chosen for comparison are the maximum range of tensile stress after Crosby et al [5] and the von Mises relationship applied to total strain range preferred by Taira et al [7]. The method used in the ASME Boiler and Pressure Vessel Code, Section III [8], is also compared to the data. To make these comparisons, the curves fitted to the uniaxial data shown in Figure 1 are used for reference purposes.

The values of range of maximum principal stress or strain at stress ratios of 1, 0.5, -0.5, and -1 for fatigue lives of 10^3, 10^4 and 10^5 cycles according to these four theories have been derived from these uniaxial data. The resulting values and comparable values interpolated from the experimental data are presented in Table 2. Contours describing the two criteria based on total strain are included in Figure 5 and describing the criterion based on stress in Figure 6. These contours are shown for one fatigue life only for simplicity. Contours for other fatigue lives are geometrically similar and so can be obtained by scaling according to the appropriate uniaxial stress or strain range.

17. MAXIMUM TENSILE STRESS AND VON MISES CRITERIA

The maximum tensile stress range criterion (Figure 6) underestimates the fatigue life for negative stress ratios throughout and for positive stress ratios at fatigue lives of 10^4 and less. At 10^4 cycles, the maximum difference from the data occurs at a stress ratio of -1 where the criterion overestimates the fatigue life by more than one hundred times.

Figure 5 shows that the von Mises criterion based on total strain range is also non-conservative over much of the range investigated. The largest differences occur with stress ratios of -1.0 and about 0.5. The differences are greater for shorter fatigue lives and for the positive stress ratios. The greatest difference of predicted fatigue lives is of the order of 100 occurring at a stress ratio of about 0.5 at 10^3 cycles.

18. CRITERION OF ASME NUCLEAR CODE

Figure 5 also shows the contour according to the ASME Nuclear Code [8]. This method of design uses a fictitious stress intensity calculated by elastic theory. This is compared to a fatigue curve, based on controlled strain uniaxial fatigue tests, containing a safety factor and a correction for mean

stress.

Only that part of the Nuclear Code which corrects for biaxiality is examined by comparison of contours in Figure 5. It is seen to be conservative at fatigue lives of 10^5 and longer and for negative stress ratios at lives longer than 10^4 cycles. The maximum divergence from the data points is for stress ratios above 0.5 at 10^3 cycles. The code underestimates the fatigue lives in this region by a factor of close to 10. The comparable factors for fatigue lives of 10^4 and 10^5 cycles are about 3 and 1 respectively. Thus use of the standard method can give unsafe designs when exceptionally few cycles are expected.

19. PROPOSED BIAXIAL CRITERION

The curves of Figure 5 corresponding to the relationship for biaxial fatigue developed in this study give better correspondence to the data than these alternative criteria. The maximum divergences from the data are at a fatigue life of 10^3 cycles under positive stress ratios. The maximum non-conservative error in life prediction is a factor of approximately 3.

The relation for biaxial fatigue developed in this paper is based on tests on mild steel and further work must be done before it can be applied generally. If this relation is found appropriate the five parameters required can be obtained from two series of principal strain controlled, fully-reversed, constant amplitude, biaxial fatigue tests in which principal strains and load are measured. Two stress ratios which might be used are uniaxial stressing and 0.5 stress ratio. The first employs standard techniques while the second can be achieved by pressurizing capped thin-walled tubular specimens from the inside and outside alternately. These two tests are relatively simple to perform, and give values of strain ratio that are well separated. A positive stress ratio is preferred to a negative stress ratio as the critical fatigue behaviour is found with a stress ratio between 0.5 and 1.

ACKNOWLEDGEMENTS

This study was supported financially by the National Research Council of Canada, grant A1694, the Defence Research Board of Canada, grant 9535-49, the University of Waterloo and the Hydro Electric Power Commission of Ontario.

REFERENCES

[1] GOUGH, H.J., "Engineering Steels under Combined Static and Cyclic Stresses", J. App. Mech., 17 (2), 113-125, (1950).

[2] FINDLEY, W.N., "Fatigue of Metals under Combinations of Stresses", Trans. ASME, 79, 1337-1348, (1957).

[3] MARIN, J., "Biaxial Tension-Tension Fatigue Strengths of Metals", J. App. Mech., 16, 383-388, (1949).

[4] SAWERT, E., "Verhalten der Baustaehle bei Wechselnder Mehrachsiger Beanspruchung", Z. Ver. Deut. Ing., 87 (39/40), 609-615 , (1943).

[5] CROSBY, J.R., BURNS, D.J., BENHAM, P.P., Effect of Stress Biaxiality on the High-Strain Fatigue Behaviour of an AL-4% Cu Alloy", Exp. Mech., 305-312, (July 1969).

[6] PASCOE, K.J., de VILLIERS, J.W.R., "Low-Cycle Fatigue of Steels under Biaxial Straining", J. Strain Anal., 2 (2), 117-126, (1967).

[7] TAIRA, S., INOUE, T., YOSHIDA, T., "Low Cycle Fatigue under Multiaxial Stresses", 11th Japan Cong. on Materials Research - Metallic Materials, 60-65, (Mar. 1968).

[8] ASME, "Criteria of the ASME Boiler and Pressure Vessel Code for Design by Analysis in Sections III and VIII, Division 2", (1969).

[9] LANGER, B.F., "Design of Pressure Vessels for Low Cycle Fatigue", Trans. ASME, J. of Bas. Eng., 389-402, (Sept. 1962).

[10] HAVARD, D.G., TOPPER, T.H., "Biaxial Fatigue of 1018 Mild Steel at Low Endurance", Proc. 1st Int. Conf. on Pressure Vessel Technology, Delft, 1267-1277, (1969).

[11] HAVARD, D.G., TOPPER, T.H., "New Equipment for Cyclic Biaxial Testing", Exp. Mech., 550-557, (Dec. 1969).

[12] TAVERNELLI, J.F., COFFIN, L.F., "Experimental Support for Generalized Equation Predicting Low Cycle Fatigue", Trans. ASME, J. Bas. Eng., 84D (4), 533-537, (1962).

[13] MANSON, S.S., "Fatigue: A Complex Subject - Some Simple Approximations", Exp. Mech., 5 (7), 193-226, (1965).

[14] BASQUIN, O.H., "The Exponential Law of Endurance Tests", Proc. ASTM, 10, 625-630, (1910).

[15] STANFIELD, G., Discussion of Paper by Gough and Pollard, Proc. I. Mech. E., 131, 93-95, (Nov. - Dec. 1935).

[16] LIBERTINY, G.Z., "Short-Life Fatigue under Combined Stress", J. Strain Anal., 2 (1), 91-95, (1967).

[17] YOKOBORI, T., YAMANOUCHI, H., YAMAMOTO, S., "Low-Cycle Fatigue of Thin-Walled Hollow Cylindrical Specimens of Mild Steel in Uniaxial and Torsional Tests at Constant Strain Amplitude", Int. J. Fracture Mech., 1, 3, (1965).

[18] OSGOOD, W.R., "Stress-Strain Formulas", J. Aero. Sci., 45-48, (Jan. 1946).

[19] HALFORD, G.R., "The Energy Required for Fatigue", J. of Mat., 1 (1), 3, (1966).

TABLE I

UNIAXIAL, TORSIONAL AND BIAXIAL FATIGUE TEST DATA

AXIAL TEST
Axial Specimens in Oil

c = -0.505
k' = 0.166
n' = 0.314

$\Delta\epsilon$ %	$\Delta\sigma$ ksi	N_f Cycles
0.198	40.6	9742500*
0.275	41.8	904493
0.385	50.4	91976
0.648	69.4	16313
0.796	75.8	13255
0.984	82.0	5634
1.465	93.0	1750
1.987	94.6	1184
2.935	103.6	540
4.11	141.4	248
6.11	152.8	97
14.06	184.4	24

AXIAL TEST
Transverse Specimens in Oil

c = -0.521
k' = 0.155
n' = 0.294

$\Delta\epsilon$ %	$\Delta\sigma$ ksi	N_f Cycles
0.344	52.1	159000
0.445	56.6	39500
0.482	57.8	41000
0.603	66.4	20667
0.761	83.2	7500
1.038	83.2	4900
1.593	88.5	1664
2.206	102.1	529
2.900	108.8	401

TORSIONAL TEST
Shear Strain Control

c = -0.406
k' = 0.589
n' = 0.271

$\Delta\epsilon_1$ %	$\Delta\sigma_1$ ksi	N_f Cycles
0.231	33.8	93362*
0.364	40.8	30299
0.414	37.1	16785
0.637	47.3	6997
0.649	40.0	4295
0.672	46.5	4575
0.756	49.8	1980
0.834	54.0	1621
0.886	50.9	1556
0.997	53.3	1545

1.21 STRESS RATIO
Circumferential Strain Control

c = -0.315
k' = 0.083
n' = 0.368

$\Delta\epsilon_2$ %	$\Delta\sigma_2$ ksi	N_f Cycles
0.189	50.0	80262
0.207	50.9	43397
0.242	55.6	24281
0.254	58.8	10400
0.259	60.1	16262
0.299	67.3	12145
0.344	71.7	2600
0.371	65.8	6965
0.403	70.7	2204

0.50 STRESS RATIO
Circumferential Strain Control

c = -0.259
k' = 0.108
n' = 0.310

$\Delta\epsilon_2$ %	$\Delta\sigma_2$ ksi	N_f Cycles
0.292	53.8	75720
0.317	58.5	42981
0.363	59.6	8660
0.371	59.3	14436
0.434	62.6	14583
0.493	69.2	5244
0.546	72.2	1632
0.623	75.1	1280

3.89 STRESS RATIO
Axial Strain Control

c = -0.332
k' = 0.172
n' = 0.572

$\Delta\epsilon_1$ %	$\Delta\sigma_1$ ksi	N_f Cycles
0.346	50.9	48162
0.415	59.7	19914
0.448	58.2	15800
0.505	73.7	10102
0.615	77.2	9788
0.702	83.8	3128

-0.34 STRESS RATIO
Circumferential Strain Control

c = -0.384
k' = 0.214
n' = 0.307

$\Delta\epsilon_2$ %	$\Delta\sigma_2$ ksi	N_f Cycles
0.348	46.8	53444
0.422	51.9	28258
0.604	60.5	11816
0.633	61.9	6498
0.693	64.2	4879
0.750	64.4	3308
0.821	67.0	2835

3.89 STRESS RATIO
Circumferential Strain Control

c = -0.375

$\Delta\epsilon_2$ %	$\Delta\sigma_2$ ksi	N_f Cycles
0.111	20.1	2190
0.179	24.0	589

-3.63 STRESS RATIO
Axial Strain Control

c = -0.443
k' = 0.219
n' = 0.207

$\Delta\epsilon_1$ %	$\Delta\sigma_1$ ksi	N_f Cycles
0.329	47.1	38900
0.513	54.3	8288

*Unbroken Specimen

TABLE II

COMPARISON OF EXPERIMENTAL DATA AND
BIAXIAL FATIGUE FAILURE CRITERIA

Values of maximum principal stress or strain range
in direction of maximum principal stress.

	Stress Ratio	FATIGUE LIFE IN CYCLES					
		10^3		10^4		10^5	
		Stress Range in ksi	Strain Range	Stress Range in ksi	Strain Range	Stress Range in ksi	Strain Range
Values Interpolated from Experimental Data	0	108.6	0.0191	73.2	0.0074	49.4	0.0033
	0.5	78	0.0064	65	0.0041	55	0.0028
	-0.5	69	0.0111	53	0.0055	41	0.0030
	-1.0	51	0.0106	42	0.0050	32	0.0027
Biaxial Fatigue Failure Criterion							
Maximum Tensile Stress	1.0	108.6	—	73.2	—	49.4	—
Von Mises using* Total Strain		—	0.0096	—	0.0037	—	0.0017
Nuclear Code		—	0.0110	—	0.0050	—	0.0023
This study (19)		85.8	0.0050	70.5	0.0039	57.9	0.0027
Maximum Tensile Stress	0.5	108.6	—	73.2	—	49.4	—
Von Mises using* Total Strain		—	0.0165	—	0.0064	—	0.0029
Nuclear Code		—	0.0150	—	0.0062	—	0.0028
This study (19)		91.0	0.0079	71.8	0.0048	56.7	0.0030
Maximum Tensile Stress	-0.5	108.6	—	73.2	—	49.4	—
Von Mises using* Total Strain		—	0.0180	—	0.0070	—	0.0031
Nuclear Code		—	0.0154	—	0.0057	—	0.0025
This study (19)		68.1	0.0111	50.1	0.0055	36.9	0.0029
Maximum Tensile Stress	-1.0	108.6	—	73.2	—	49.4	—
Von Mises using* Total Strain		—	0.0165	—	0.0064	—	0.0029
Nuclear Code		—	0.0136	—	0.0049	—	0.0021
This study (19)		51.2	0.0097	38.1	0.0049	28.3	0.0026

* Using 0.5 Poisson's ratio

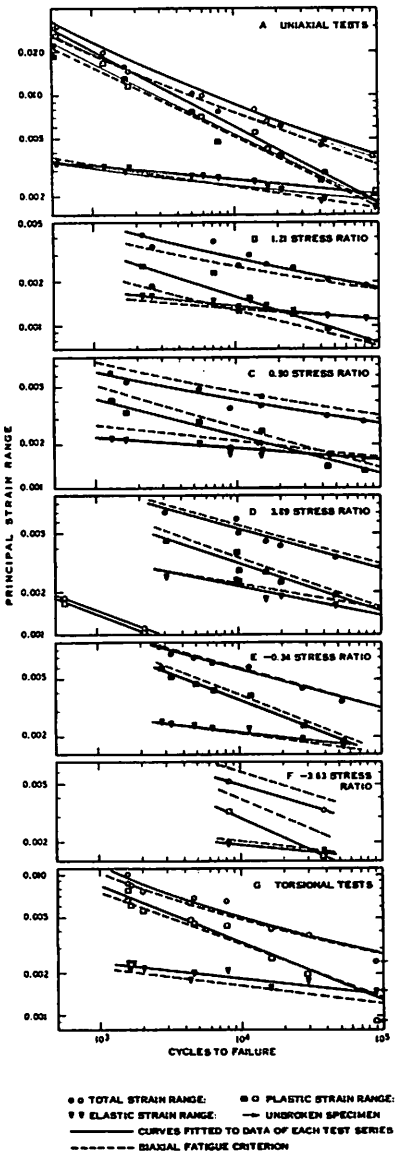

1. UNIAXIAL, TORSIONAL AND BIAXIAL FATIGUE DATA
   Total, Plastic and Elastic Ranges of Controlled Strain versus Fatigue Life

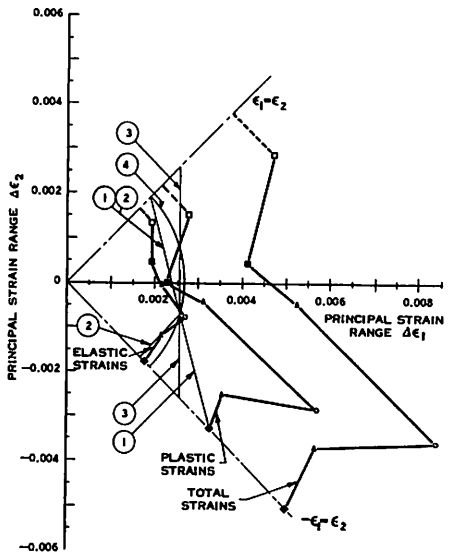

SYMBOL	□	■	△	○	△	◆
STRESS RATIO	1.21	0.50	3.89	∞	−0.34	−1.00

2. EQUAL FATIGUE LIFE CONTOURS AT 10^4 CYCLES
   Based on Total, Plastic and Elastic Strain Data
   Failure Criteria included for Reference are:
   1. Maximum Principal Stress
   2. Maximum Shear Stress
   3. Maximum Strain
   4. Distortion Strain Energy

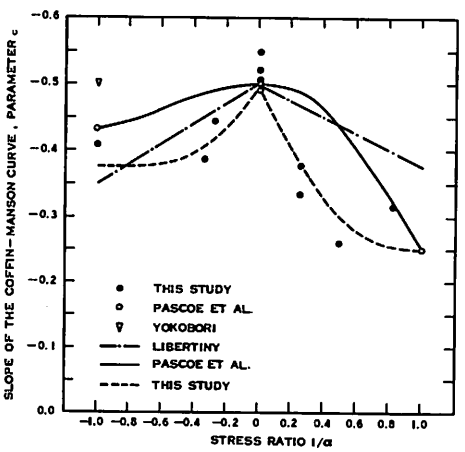

3. VARIATION OF SLOPE OF COFFIN-MANSON CURVE WITH STRESS RATIO

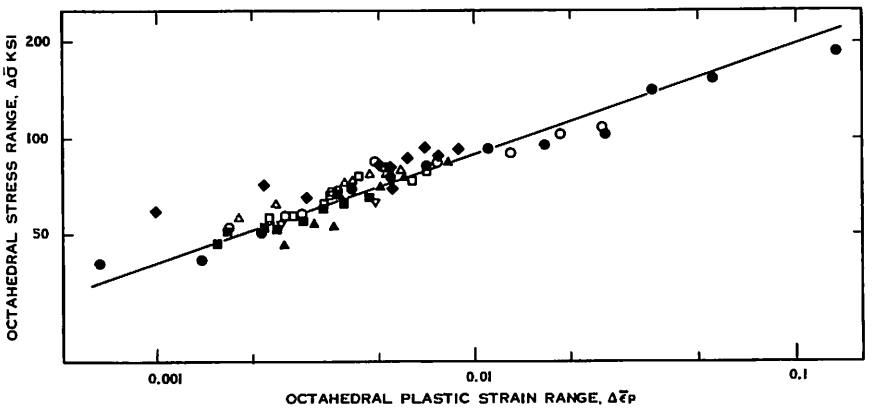

SYMBOL	○	●	□	■	▲	▽	△	◆
STRESS RATIO	∞	0	1.21	0.50	3.89	−3.63	−0.34	−1.00

4. NORMALIZED CYCLIC STRESS-STRAIN CURVE

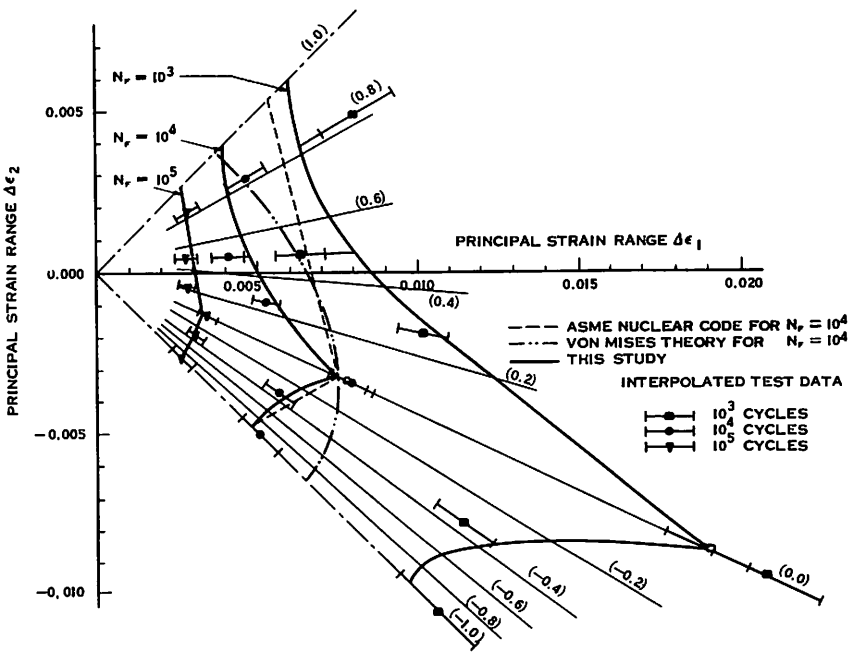

5. BIAXIAL FATIGUE RELATION FOR MILD STEEL
Equal Fatigue Life Contours Based on Total Strain Range
Stress ratios shown in brackets. Fatigue lives in cycles.

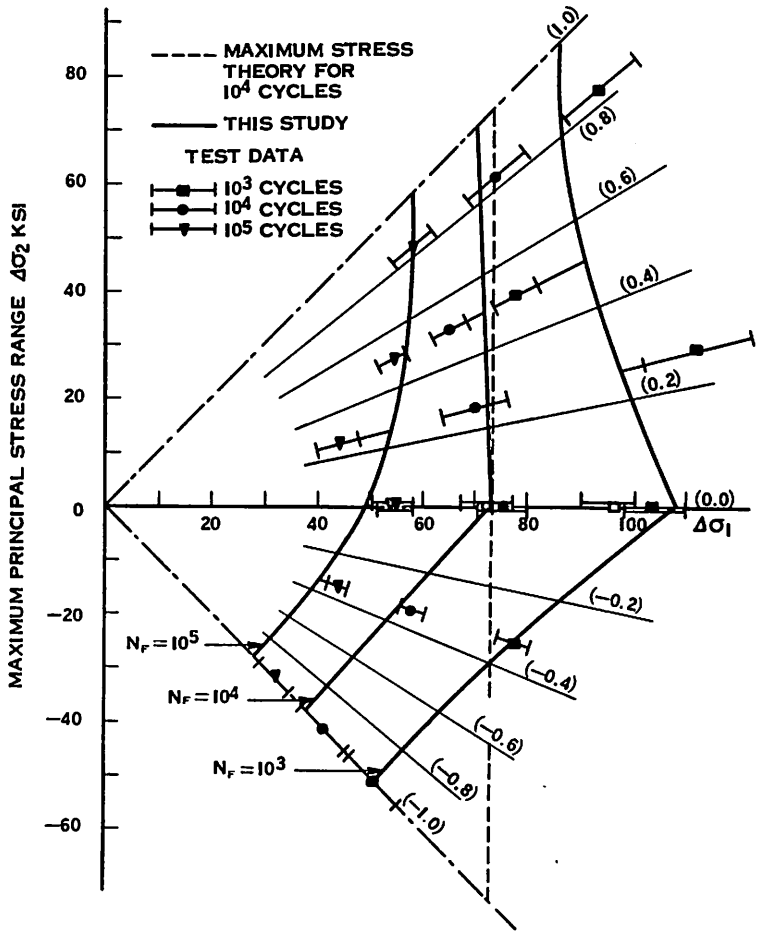

6. BIAXIAL FATIGUE RELATION FOR MILD STEEL
Equal Fatigue Life Contours Based on Stable Stress Range
Stress ratios shown in brackets. Fatigue lives in cycles.

DISCUSSION

Q E. KREMPL, U. S. A.

The criterion used to best correlate the result is sensitive to superposed hydrostatic pressure. This correlation supports the fact that the fatigue phenomenon is different from yielding as it is sensitive to superposed pressure. Therefore, no yield criteria should be used for the correlation of fatigue data.

A D. G. HAVARD, Canada

The criterion developed shows the fatigue failures to be sensitive to the average of the applied stresses (hydrostatic stress) as well as to the maximum difference between principal stresses. There was no mean pressure in the tests performed as fully reversed strain control was used, however the form of the criterion strongly suggests sensitivity to mean pressure.

The endurance limit under biaxial stressing has been experimentally shown, for ductile metals, to depend on stress ratio in a similar manner to yielding. However yielding and fatigue are indeed significantly different phenomena and theoretical contraints on the form of the yielding relationships (such as concavity) do not apply to fatigue relationships.

Q G. HILLS, U. K.

I note the last slide you have shown was not included as a figure in the printed paper. It is this diagram, giving a comparison with the ASME code, that I would wish to comment on.

In using the ASME code, account of biaxial stresses in fatigue is considered by using "stress intensity" when entering the fatigue curve. The ASME code therefore allows for a biaxial condition according to the Tresca criterion.

Has your comparison taken account of this knowledge ?

A D. G. HAVARD, Canada

The last slide shown is presented here for reference. It depicts the fatigue data obtained superimposed upon the ASME pressure vessel code, Section III curve for design against fatigue. The experimental data have been reduced to equivalent values of S_A (or "stress intensity") using the procedure suggested in the code for use in design. The code is in fact based on strain controlled fatigue data converted to "stress" units by the use of a modulus value. As such the maximum difference in these "stresses" is not truly the Tresca criterion but some modification of it. It is included in the contours shown in Fig. 5 of the paper.

The new figure presented here shows that the design curve of the pressure vessel code retains conservatism over the data points but with a significant reduction in safety factor, particularly for positive stress ratios at the shortest lives studied (10^3-10^4 cycles). Modifications

that might be introduced, based on the criterion developed in this paper and a safety factor of close to 2 on the data points are indicated by dashed lines below the code design curve.

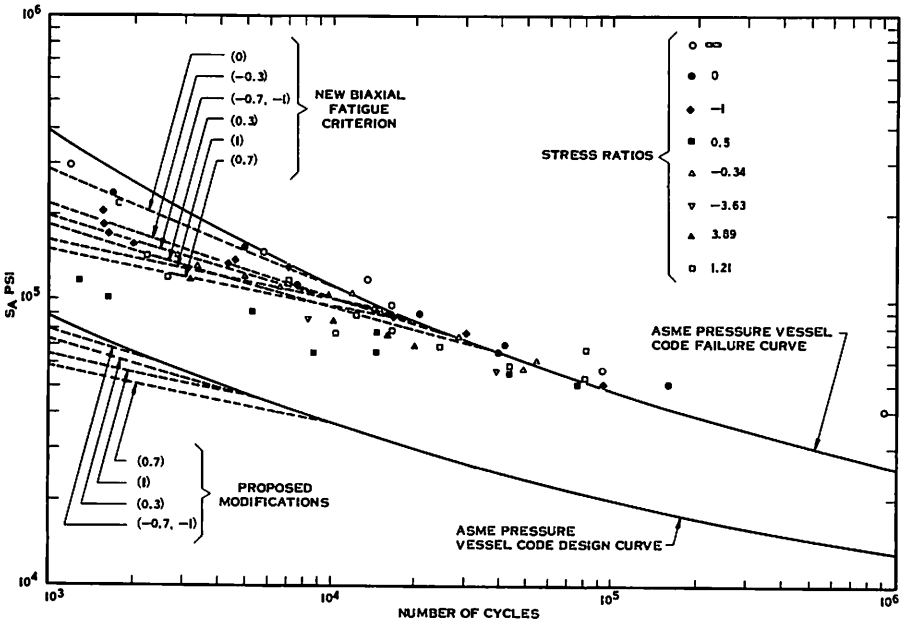

Fig. 7 - Comparison of ASME pressure vessel code fatigue failure and design curves with biaxial fatigue test data.

Including curves representing the biaxial fatigue criterion and proposed modifications to the code design curve for various biaxial stress ratios (shown in brackets).

Q R. J. DOHRMANN, U. S. A.

In the reporting of your fatigue data what criterion of failure was used and how was it determined and measured ?

A D. G. HAVARD, Canada

The fatigue tests were terminated when the presence of a small crack was detected through a distortion of the hysteresis (stress-strain) loop that was observed on an oscilloscope or a plotter throughout these tests. This distortion corresponded to a small drop in load due to a minor crack. It is therefore considered that the end point represents all of the stages of deterioration up to crack initiation and some small part of the crack propagation stage.